

59

N 9 1 - 3 0 2 1 3

PHOTOREFLECTANCE AND DLTS EVALUATION OF PLASMA-INDUCED DAMAGE
IN GaAs AND InP PRIOR TO SOLAR CELL FABRICATION

L. He and W.A. Anderson
State University of New York at Buffalo
Center for Electronic and Electro-optic Materials
Department of Electrical and Computer Engineering
Bonner Hall, Amherst, NY 14260

ABSTRACT

This study considers the effect of plasma etching on both GaAs and InP followed by damage removal using rapid thermal annealing (RTA). Effects of these processes were studied by photoreflectance spectroscopy (PR) and deep level transient spectroscopy (DLTS). These techniques are useful in evaluation of wafers prior to and effects of plasma processing during solar cell fabrication.

Wafers examined in this study included GaAs with $N_D = 5 \times 10^{17} \text{ cm}^{-3}$, undoped (u) InP with $n = 5 \times 10^{15} \text{ cm}^{-3}$, InP with $N_D = 4 \times 10^{17} \text{ cm}^{-3}$ and InP with $N_A = 1 \times 10^{16} \text{ cm}^{-3}$. Samples were taken from these wafers for an initial study of PR and DLTS using Au-Schottky contacts. Some samples were then plasma etched in CF_4 gas using conditions of 50-150W and a pressure of 10-100 m Torr. Some of these were processed by RTA at 450°C for 10s to remove plasma damage. PR data showed energy gap (E_g) to decrease by 0.006 eV after plasma etching for n-GaAs and u-InP. E_g recovered completely after plasma etching. PR also showed the appearance of defect-related extraneous signals after plasma etching which were removed by RTA. DLTS revealed the addition of new defects after plasma etching which were later removed by RTA. For example, defects in n-GaAs with activation energy of 0.38 eV, 0.57 eV and 0.67 eV were proven to be surface related by the shift in DLTS signal with fill pulse height. These signals disappeared completely following RTA.

INTRODUCTION

Plasma etching is widely used in semiconductor technology to form fine surface structures. It has the advantages of selectivity, precision and versatility. In photovoltaic devices, plasma etching may permit selective diffusion or ion implantation, perhaps for the region underneath grid lines. It may also be used to form openings in passivation layers such that fine grid contacts may be formed. This study considers the effect of plasma etching on both GaAs and InP followed by damage removal using rapid thermal annealing (RTA). Effects of these processes were studied by photoreflectance spectroscopy (PR) and deep level transient spectroscopy (DLTS). PR is proven to be an effective non-destructive tool in evaluating processed wafers prior to final solar cell fabrication.

Plasma dry etching is used for fabrication of GaAs-based electronic and photonic devices and their integration (refs. 1-2). Its advantages in high resolution, anisotropic processing and controllability have been clearly demonstrated. Plasma etching inherently induces damage, which may affect various surface properties of the substrate. Contamination originating from polymer formation during etching or materials sputtered from the etching chamber can also influence device performance. A number of reports have been made on the investigation of different cases of plasma induced damage (refs. 3-8). Damage has been observed and compared in GaAs by sputter etching and ion beam etching. The characterization techniques most widely used include deep level transient spectroscopy (DLTS) and more recently, photoluminescence (PL). The removal of plasma induced damage has also been discussed by some authors. In this paper we report the study of reactive ion etching in CF_4 performed in a parallel plate reactor for GaAs, particularly in terms of chamber pressure and power. Photorefectance spectroscopy (PR) was used to evaluate the sample surface electrical and optical properties in a nondestructive manner (refs. 10-13). Rapid thermal annealing (RTA) was conducted for a study of the plasma induced damage removal. The effect of plasma etching on device characteristics was studied by evaluating Schottky diodes fabricated on the plasma etched material surfaces. Deep level transient spectroscopy (DLTS) was used to detect and characterize trap centers.

Much less work has been conducted on InP. Our work is also of a preliminary nature but includes both PR and DLTS data for studies of the initial wafer, effects of plasma etching and the healing produced by RTA.

EXPERIMENTAL

The samples used in this work were (100) n-GaAs with doping (N_d) of about $2.5 \times 10^{17}/\text{cm}^3$. Chemical etching in $\text{H}_3\text{PO}_4:\text{H}_2\text{O}_2:\text{H}_2\text{O} = 3:1:100$ for 8 seconds and $\text{HCl}:\text{H}_2\text{O} = 1:1$ for 1 minute were performed to remove an initial damaged surface and native oxide layer. Ohmic contacts were first applied to the back of the wafers by AuGe/Ni evaporation. A 450°C , 10 seconds RTA was conducted for the ohmic contact formation. After RTA treatment, the starting wafer was sectioned. One of the pieces was directly taken for PR measurement. The others were plasma etched with the process under study. The plasma etched samples were labeled as G1, G2 and G3 following in sequences of 10mTorr/50W, 50mTorr/100W and 100mTorr/150W plasma etching conditions. Each separately etched wafer was then cut into halves. One half was immediately loaded into a vacuum chamber for Schottky Au deposition. Another half was first taken for PR testing followed by a $450^\circ\text{C}/10\text{s}$ RTA treatment to remove plasma induced damage. Finally, Schottky metal was deposited as in the other samples. Correspondingly, after RTA removal of plasma induced damage, 3 samples were labeled as GR1, GR2 and GR3, respectively. Measurement was also conducted on a starting wafer which was labeled G0.

Undoped InP ($n = 5 \times 10^{15}/\text{cm}^3$), n-type doped InP ($N_D = 4 \times 10^{17}/\text{cm}^3$), and p-type doped InP ($N_A = 1 \times 10^{16}/\text{cm}^3$) wafers were also used in this study. In the plasma etching, a CF_4 gas was used with an etching time of 2 minutes. Plasma etching was conducted in a Varian RF-diode sputtering system. RTA was conducted with a commercial RTA HEATPULSE 210 in a nitrogen atmosphere at 360°C for 10s. A standard arrangement of PR apparatus was used to measure PR on the starting wafer, after plasma etching and after RTA. A detailed description of the PR set-up was presented elsewhere (ref. 11).

RESULTS AND DISCUSSION

A. Gallium Arsenide

According to Aspnes' theory (ref. 12), the parameters of the GaAs layer used in this study would have the PR spectra near bandedge in the high field limit. Thus, the PR signal is an expression of the product of Airy functions and their derivatives which shows the asymptotic form:

$$\Delta R/R \sim \cos\{(2/3)[(\hbar\omega - E_g)/\hbar\Omega]^{3/2} - \pi(d-1)/4\} \quad (1)$$

where $\hbar\omega$ is the energy of the probe beam, E_g is the energy of the bandgap, $\hbar\Omega$ is the characteristic energy of a quantum mechanical particle of interband reduced mass μ being accelerated by the electric field, F_s

$$\hbar\Omega = (e^2 F_s^2 \hbar^2 / 8\mu)^{1/3} \quad (2)$$

Here, d is the dimensionality of the critical point. For a direct transition on GaAs, $d = 3$ (ref.13).

Figure 1 shows the PR spectra from the starting GaAs wafer and plasma etched samples. Significant PR spectra inflection was observed from plasma etched samples. The large features around the bandgap energy region arise from excitonic effects in the surface space charge region (SCR) (ref. 13). FKO was clearly shown in most samples which are related to the surface electric field as mentioned above. In Fig. 1 (b), (c) and (d) are plotted the PR spectra immediately after plasma etching with chamber pressures of 10mTorr, 50mTorr and 100mTorr. The starting wafer G0, shown in Fig.1 (a), has the strongest PR signal which implies good crystal structure perfection (ref. 14). From the FKO period, a F_s of 2.25×10^5 V/cm was obtained from G0. The PR spectrum from G1 is shown in Fig.1 (b). PR signal amplitude was decreased about 60% and FKO could not be seen. Both phenomena showed the introduction of crystal imperfection by plasma etching. Displayed in Fig.1 (c) is the PR of G2 where FKO were observed and a F_s of 1.29×10^5 V/cm was calculated. Fig.1(d) shows the PR from sample G3. Figs.1(c) and (d) showed decreased PR signal amplitude compared with the starting wafer Fig.1(a). Several features at energy lower than bandgap energy position (labeled as T1, T2) were clearly shown. We consider these features to come from plasma etching-induced damage.

Fig. 2 shows the PR spectra of the samples GR1, GR2 and GR3 which were G1, G2 and G3 after RTA treatment, respectively. It is obvious that RTA treatment eliminated or reduced plasma induced damage. The PR signal amplitudes were increased for all samples and the spectra shapes became similar to those for the starting wafer. In particular, Figs.2 (b) and (c) are almost exact copies of Fig.1 (a). FKO were observed in all three RTA treated samples giving F_s values of 1.63×10^5 V/cm, 1.76×10^5 V/cm and 2.43×10^5 V/cm for GR1, GR2 and GR3, respectively.

B. DLTS analysis

Figure 3 shows the DLTS spectra from the starting wafer G0 (solid line) and for comparison purpose, from one of the plasma etched sample G3 (dashed line). Two traps were

detected in the starting wafer. One labeled E1 with activation energy $E_a = 0.83\text{eV}$, capture cross section $\sigma = 2.1\text{-}2.8 \times 10^{-13}\text{ cm}^2$ and trap concentration $N_t = 3\text{-}4 \times 10^{14}/\text{cm}^3$ at bias voltage $V_r = 2\text{V}$, and FPH = 0.5V. We consider this trap to be the well known residual defect in bulk GaAs material as EL2 (ref. 15). Another trap labeled E2 was found with $E_a = 0.16\text{-}0.17\text{eV}$, $\sigma = 1.25\text{-}2.25 \times 10^{-16}\text{ cm}^2$, and $N_t = 3\text{-}4 \times 10^{14}/\text{cm}^3$. By changing bias and FPH amplitude, the DLTS peak position did not show an apparent shift which indicated these traps in G0 to be in the bulk arising from the material growth process. A plasma induced trap peak in G3 is also shown in Fig. 3 which is more than one order higher in trap concentration compared with those traps found in G0.

Figure 4 is a typical DLTS spectra from sample G2. The detected trap was clearly observed in all 6 different rate windows. Figure 5 shows DLTS spectra from plasma etched samples G1, G2 and G3 under the same testing conditions. One trap peak in a temperature range between 320°K and 360°K was detected in every sample. In the spectra shown, this plasma-induced trap peak was dominant since it has a much higher trap concentration than those in the starting wafer. Values of E_a , σ , and N_t were calculated and are summarized in Table 1. For 10mTorr/50W plasma etching of sample G1, a trap with $E_a = 0.38\text{eV}$, $\sigma = 1.25 \times 10^{-17}\text{ cm}^2$ and $N_t = 1.6 \times 10^{16}/\text{cm}^3$ was found under 2V bias and 0.5V FPH. For the same DLTS condition, a trap with $E_a = 0.57\text{eV}$, $\sigma = 4.65 \times 10^{-15}\text{ cm}^2$, and $N_t = 1.2 \times 10^{16}/\text{cm}^3$, and with $E_a = 0.67\text{eV}$, $\sigma = 2.03 \times 10^{-13}\text{ cm}^2$ $N_t = 5.4 \times 10^{15}/\text{cm}^3$ were detected for the 50mTorr/100W (G2) and 100mTorr/150W (G3) plasma etching conditions, respectively. Conditions used for sample G3 are obviously preferred. Figure 6 shows DLTS spectra from sample G2 under different conditions of fill pulse height(FPH). The trap peak shifting can be clearly seen. As the FPH value increased, the peak position shifted to the lower temperature side. Similar results were obtained from G1 and G3. This shows these plasma induced traps to be interface traps.

The activation energies of induced traps are related to plasma etching pressure and power. Data showed the activation energy to increase with the pressure and power during the plasma etching. This suggests that the higher pressure and power, which increases the plasma particle density participating in collision with the substrate, creates deeper trap levels. The detailed mechanism of the activation energy deviation is under investigation. Arrhenius plots of the thermal emission rates of the deep electron levels found in plasma etched GaAs are presented in Figure 7. The reduction of induced deep levels by RTA annealing was effective. Only one trap, E2, in the starting wafer, was observed in GR1. All plasma induced trap levels disappeared after RTA treatment.

B. Indium Phosphide

Very pronounced FKO was observed in p-type doped InP after plasma etching and RTA as shown in Fig. 8. The PR from the starting wafer is given in Fig. 8(a) where the PR signal was quite weak and FKO was absent. After plasma etching, a pronounced FKO was achieved and the PR signal became very strong. The weak PR signal in the starting wafer may come from an initial oxidation layer which was effectively removed after plasma etching. A F_s of $2.74 \times 10^4\text{ V/cm}$ was obtained. After RTA treatment at 360°C/10s, good FKO were still observed and the shape of the PR was similar to that before RTA. The bandgap transition shifted to the higher energy side and a higher surface electric field F_s of 4.13×10^4 was obtained.

Figure 9 shows the PR spectra of an n-type doped InP sample. No obvious FKO was observed here. The PR modulation in the near bandgap region was obtained from every spectrum which permits the bandgap energy to be determined by Aspnes' method. A lower energy side peak labeled T_0 , with energy position at 1.210 eV, was observed in all PR spectra which may come from impurity or structural defect modulation. Other authors concluded the low energy side peak to be associated with doping inhomogeneities in the samples (ref. 17). Another PR maximum peak occurred on the higher energy side labeled O_1 in Figure 9 with energy position at 1.417 eV. After the plasma treatment, the higher energy peak disappeared which implied that O_1 came from a kind of surface oxidation layer which could be removed by the plasma etching. A new peak with energy position at 1.280 eV, labeled T_1 , appeared after plasma etching which should come from the plasma damage. The current RTA treatment on n-type InP ($360^\circ\text{C}/10\text{s}$) could not remove both T_0 and T_1 . But, the PR signal became stronger after RTA which indicated the partial recovery of the crystal structure damage (ref. 18). It was found that the higher energy side peak O_1 reoccurred after RTA which may be attributed to a newly grown oxidation layer.

Figure 10 shows the PR spectra of undoped(n-type) InP material. An extra peak at energy below bandgap with position at 1.258 eV, labeled T_0 , was observed in all PR spectra which may arise from impurity or defect modulation as found in the n-type doped InP. Another peak, labeled T_1 , occurred in the plasma treated sample with energy position at 1.305 eV which was introduced by the plasma etching. Different RTA conditions were used for undoped InP which include: $360^\circ\text{C}/10\text{s}$, $390^\circ\text{C}/10\text{s}$, $390^\circ\text{C}/20\text{s}$, and $420^\circ\text{C}/10\text{s}$. After the $390^\circ\text{C}/20\text{s}$ RTA treatment, E_g shifted back to 1.344 eV and the T_1 peak diminished which showed this annealing condition to effectively recover the crystal imperfection and damage due to the plasma. The energy peak T_0 kept occurring in all PR spectra, at the same position and intensity, which shows that it could not be influenced by plasma and RTA. We also noticed that the PR signal became weaker after plasma treatment which showed that the plasma processing did introduce a disordered region and affected crystal perfection.

CONCLUSIONS

Both photoreflectance (PR) and deep level transient spectroscopy (DLTS) are effective in evaluating quality of starting wafers and defects introduced by plasma etching. Photoreflectance is particularly valuable because of the non-destructive nature of the test. Both PR and DLTS reveal damage signals after plasma etch with DLTS giving traps having activation energy dependent on plasma condition. Studies on GaAs reveal an almost complete healing of plasma-induced defects after RTA at 450°C for 10s. The degree of damage induced by plasma etch may be controlled by variation of the power and pressure during plasma etching. Thus, an optimum condition may be achieved.

Similar studies on InP revealed a much greater sensitivity to plasma etching such that samples could not be tested by DLTS after plasma etching although a PR signal could be seen. Complete recovery after RTA was not observed. InP also exhibited extraneous PR signals both above and below E_g indicating inherent defects as well as plasma induced ones. Similar defects have been seen by others but have not been clearly identified.

REFERENCES

- 1.L.A. Coldren, K. Iga, B. I. Miller and J.A. Rentschler, Appl. Phys. Lett., 37, 681 (1980).
- 2.S. Semmra, T. Ohta, T. Kwroda and H. Nakashima, Jpn. J. Appl. Phys., 24, L463 (1985).
- 3.K. Asakawa and S. Sugata, J. Vac. Sci. Tech., B3, 402 (1985).
- 4.S.W. Pang, J. Electrochem. Soc.: Solid-State Sci. & Technol., 133, 784 (1980).
- 5.S.W. Pang, G.A. Lincoln, R.W. McClelland, P.d. DeGraff, M.W. Geis and W.J. Piacentini, J. Vac. Sci. & Technol., B1, 1334 (1983).
- 6.Y. Yuba, T. Ishida, K. Gamo and S. Namba, J. Vac. Sci. & Technol., B6, 253 (1988).
- 7.J.Z. Yu, N. Masui, Y. Yuba, T. Hara, M. Hamagaki, Y. Aoyagi, K. Gamo and S. Namba, Jpn.J. Appl. Phys., 28, 2391 (1989).
- 8.S. Sugata and K. Asakawa, J. Vac. Sci & Technol., B6, 876 (1988).
- 9.F.H. Pollak and H. Shen, J. Elect. Mat., 19, 399 (1990).
- 10.H. Shen, F.H. Pollak and J.M. Woodall, J. Vac. Sci. Technol. B8, 413 (1990).
- 11.L.He and W. A. Anderson, J. Elect. Mat., 20, 359 (1991).
- 12.D.E. Aspnes, Proc. 1st Int. Conf. on Modulation Spectroscopy,1972, [surf. Sci. 37, 418 (1973)].
- 13.M. Sydor, N. Jahren, W.C. Mitchel, W.V. Lampert, T.W. Haas, M. Y. Yen, S.M. Mudare and D.H. Tomich, J. Appl. Phys., 67, 7423 (1990).
- 14.N. Bottka, D.K. Gaskill, R.S. Sillmon, R. Henry and R. Glosser, J. Elect. Mat., 17, 161 (1988).
- 15.D.W.E. Allsopp, Solid State Phenomena, 1 & 2, 211 (1988).
- 16.K. Yamasaki, M. Yoshida and T. Sugano, Jpn. J Appl. Phys., 18, 113 (1979).
- 17.M. Gal, R. Shi and J. Tann, J. Appl. Phys., 66, 6196 (1989).
- 18.S.K. Brierley and D. S. Lehr, J. Appl. Phys., 67, 3878 (1990).

Table 1 Data from DLTS Studies of GaAs
 (@ Vr = -2V, FPH = 0.5V)

Sample	Activation Energy E_a (eV)	Capture Cross-Section σ (cm ²)	Trap Density N_t (cm ⁻³)
G0	0.83	2.80×10^{-13}	3.0×10^{14}
	0.16	1.25×10^{-16}	4.0×10^{14}
G1	0.38	1.25×10^{-17}	1.6×10^{16}
G2	0.57	4.65×10^{-15}	1.2×10^{16}
G3	0.67	2.03×10^{-13}	5.4×10^{15}

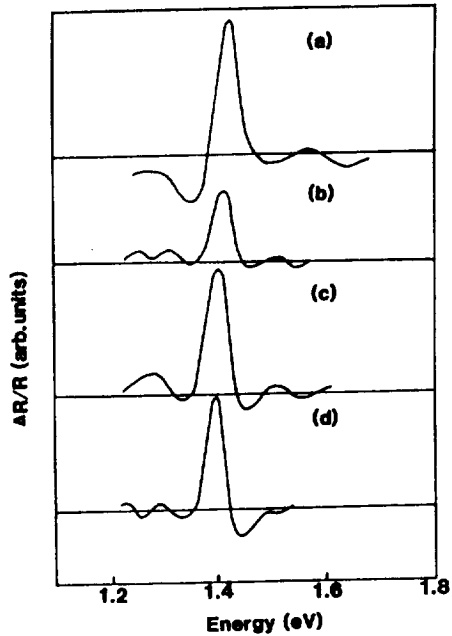


Fig. 1 The PR spectra of (a) starting wafer, and after plasma etching at (b) 10m Torr/50W, (c) 50mTorr/100W, (d) 100mTorr/150W.

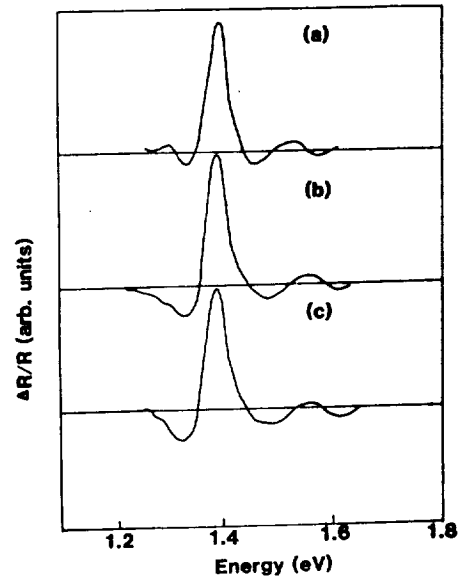


Fig. 2 The PR spectra from plasma etched samples (a) 10mTorr/50W, (b) 50mTorr/100W and (c) 100mTorr/150W, all after RTA treatment at 450°C, 10 seconds.

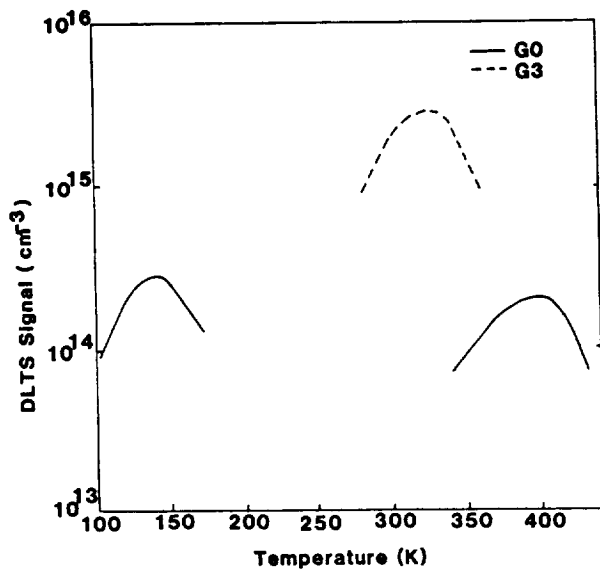


Fig. 3 DLTS spectra for the starting GaAs wafer G0 (solid line) and plasma etched sample G3 where the dashed line shows the added signal.

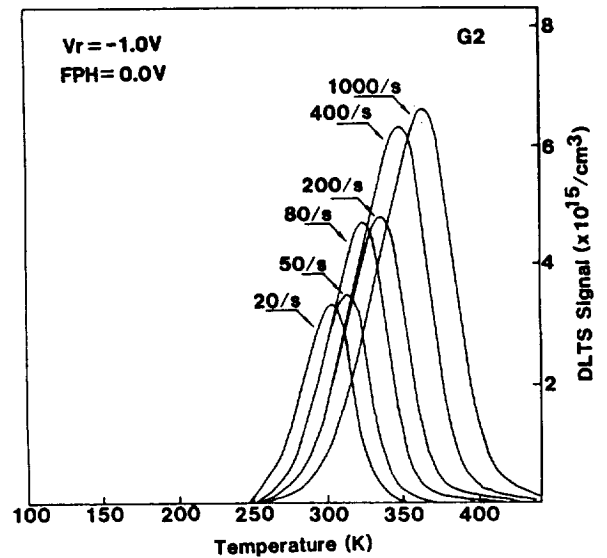


Fig. 4 A typical DLTS spectra of sample G2 (50mTorr/100W plasma etched) for different rate windows.

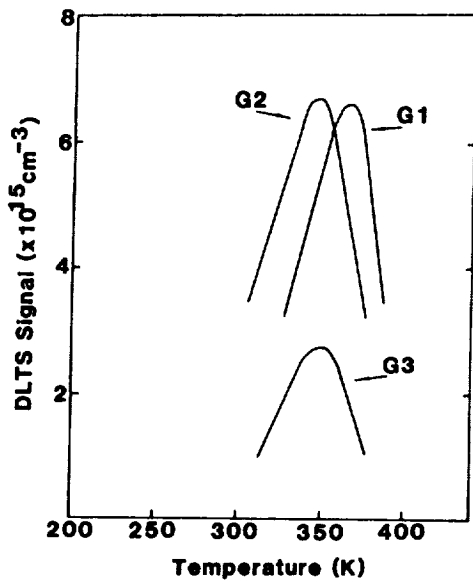


Fig. 5 The DLTS spectra from samples G1, G2 and G3 under the same testing conditions.

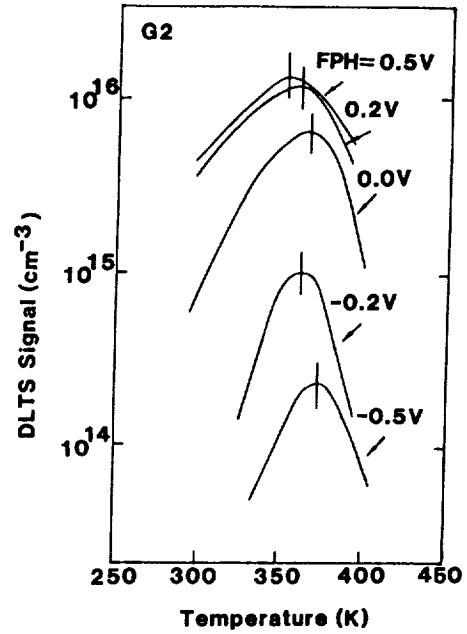


Fig. 6 The DLTS spectra from sample G2 under different fill pulse height (FPH).

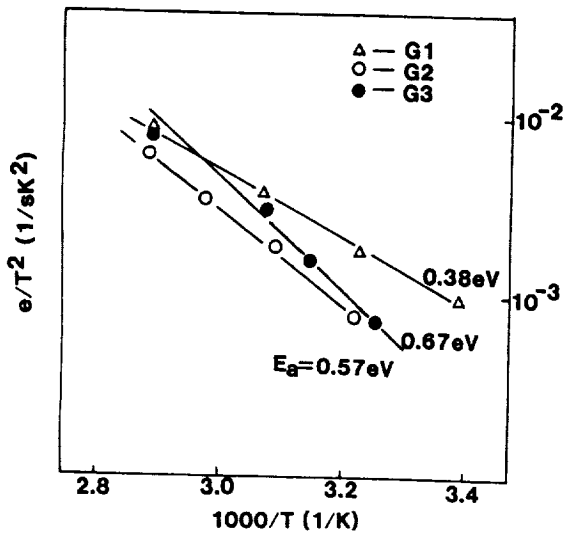


Fig. 7 Arrhenius plots of the thermal emission rates of the electron traps found in plasma etched GaAs samples G1, G2 and G3.

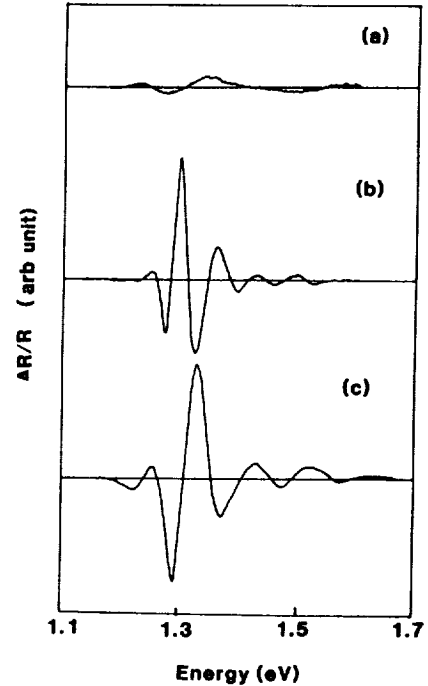


Fig. 8 PR spectra from a p-type InP from (a) starting wafer and the wafer after: (b) plasma etching, (c) RTA.

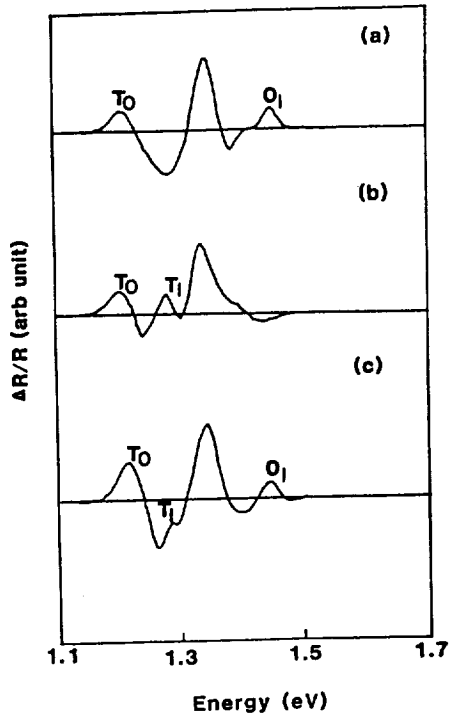


Fig. 9 PR spectra of n-type doped InP.
 (a) starting wafer (b) plasma etched
 and (c) RTA treated wafer.

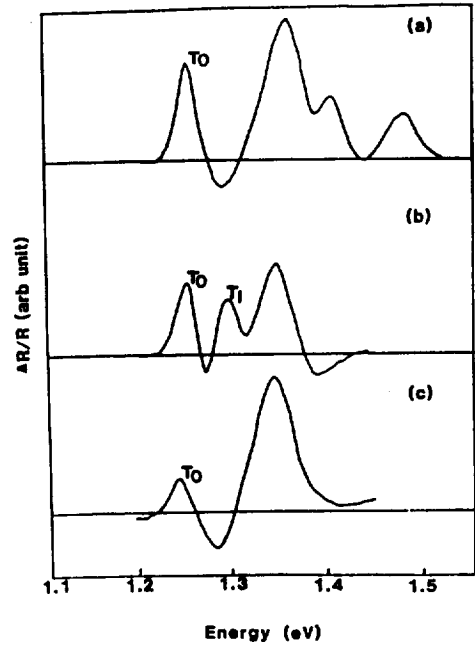


Fig.10 PR spectra of undoped InP.
 (a) starting wafer (b) plasma etched
 and (c) RTA treated wafer.

